

Optimized mechanical quadrature squeezing beyond the 3 dB limit via gradient-descent algorithm

Yu-Hong Liu¹ and Jie-Qiao Liao^{1,2,*}

¹*Key Laboratory of Low-Dimensional Quantum Structures and Quantum Control of Ministry of Education,
Key Laboratory for Matter Microstructure and Function of Hunan Province,
Department of Physics and Synergetic Innovation Center for Quantum Effects and Applications,
Hunan Normal University, Changsha, 410081, China*

²*Institute of Interdisciplinary Studies, Hunan Normal University, Changsha, 410081, China*

(Dated: May 21, 2024)

The preparation of mechanical quadrature-squeezed states holds significant importance in cavity optomechanics because the squeezed states have extensive applications in understanding fundamental quantum mechanics and exploiting modern quantum technology. Here, we propose a reliable scheme for generating mechanical quadrature squeezing in a typical cavity optomechanical system via seeking for optimal cavity-field driving pulses using the gradient-descent algorithm. We realize strong quadrature squeezing in a mechanical resonator that exceeds the 3 dB steady-state limit, even with a thermal phonon occupancy of one hundred. Furthermore, the mechanical squeezing can be ultrafastly created within one mechanical oscillation period. We also obtain the optimal pulsed drivings associated with the created mechanical squeezings and analyze the mechanism for mechanical squeezing generation. This work will promote the application of optimal quantum control in quantum optics and quantum information science.

I. INTRODUCTION

Cavity optomechanics [1] is a frontier research field focusing on the radiation-pressure interaction between cavity fields and moving mirrors at macroscopic scales. Owing to the nonlinear properties of the optomechanical interaction and the development of laser cooling techniques [2–5], optomechanical systems provide new paths and opportunities for generation and manipulation of macroscopic nonclassical states, such as entangled states [6–11], quantum superposed states [12–15], and squeezed states of fields [16–21] and mechanical resonators [22–44].

Quantum squeezing, as an essential quantum resource, plays an increasingly significant role in modern quantum technology ranging from quantum precision measurement to quantum information processing [45, 46]. Quantum squeezing of mechanical modes holds significance as it has the potential to enhance the accuracy of quantum measurements [47]. There exist many theoretical and experimental schemes for generating mechanical squeezing based on various methods, such as parametric squeezing [24–31], quantum measurement [32–36], quantum state transfer [37–39], mechanical nonlinearities [24, 40, 41], and reservoir engineering [43, 44]. Although great advances have been made in squeezing generation, how to generate mechanical squeezing beyond the 3 dB limit [26, 38, 48] in a typical optomechanical system is still an important and desired task in this field. In addition, from the view point of realistic application, an ultrafast generation of strong mechanical squeezing remains a challenge.

In cavity optomechanical systems, the external optical driving provides an effective way to control the quantum properties and dynamical behaviors of the system [25, 27, 49–51]. The design of an optimal optical driving to achieve a supposed goal is an interesting topic in this system. Currently, quantum control techniques have been successfully applied to various schemes in cavity optomechanical systems [52], such as robust state transfer [53], optimized cooling [54–56], entanglement enhancement [57, 58], and strong squeezing [59, 60]. Furthermore, optimal control technology based on the gradient-descent algorithm [61] has been recognized as a powerful method to accomplish complex control tasks, and hence it is expected to provide new ways to optimize the control of cavity optomechanical systems.

In this paper, we apply the gradient-descent algorithm to prepare mechanical quadrature squeezing in a typical cavity optomechanical system. Our scheme can break the 3 dB steady-state squeezing limit even when the environment thermal phonon occupation associated with the mechanical resonator reaches the order of one hundred. The mechanical quadrature squeezing is achieved by designing a proper pulsed driving to the cavity field. Concretely, we use the gradient-descent algorithm to iteratively optimize the pulsed driving for achieving strong mechanical squeezing. The optimal waveforms of the pulsed driving amplitude and phase are also obtained. In particular, mechanical squeezing can be ultrafastly prepared within one mechanical oscillation period, providing more chance for realistic applications of the generated squeezing before decoherence. Our method will encourage further researches on optimal quantum control in cavity optomechanical systems.

The rest of this paper is organized as follows. In Sec. II, we introduce the Hamiltonians and present the equations of motion. In Sec. III, we show the generation of me-

* Corresponding author: jqiao@hunnu.edu.cn

chanical quadrature squeezing using the gradient-descent algorithm. In Sec. IV, we present some discussions on the physical mechanism and experimental implementation of this scheme and conclude this work. An Appendix is presented to show the derivation of the variation $\delta[\Delta X_b^2(\theta, T)]/\delta Q_m$ used in the gradient-descent algorithm.

II. HAMILTONIANS AND EQUATIONS OF MOTION

We consider a typical cavity optomechanical system that consists of a mechanical resonator optomechanically coupled to a single-mode cavity field. To control the dynamics of the system, the cavity mode is driven by a strong pulsed field with carrier frequency ω_L , driving amplitude $\Omega(t)$, and driving phase $\phi(t)$. In a rotating frame defined by the unitary operator $\exp(-i\omega_L t a^\dagger a)$, the Hamiltonian of the system reads ($\hbar = 1$)

$$H_{\text{opt}}(t) = \Delta_c a^\dagger a + \omega_m b^\dagger b - g_0 a^\dagger a (b^\dagger + b) + [\Omega(t)e^{-i\phi(t)} a^\dagger + \text{H.c.}], \quad (1)$$

where a^\dagger (a) and b^\dagger (b) are, respectively, the creation (annihilation) operators of the cavity field and the mechanical resonator, with the corresponding resonance frequencies ω_c and ω_m . The $\Delta_c = \omega_c - \omega_L$ is the detuning of the cavity-field resonance frequency with respect to the pulsed-field carrier frequency. The g_0 term describes the radiation-pressure coupling between the cavity field and the mechanical resonator, with g_0 being the single-photon optomechanical-coupling strength.

In the open-system case, we assume that the cavity field is coupled to a vacuum bath, while the mechanical resonator is connected to a heat bath. Considering the Markovian dissipations, the evolution of the system is governed by the quantum master equation

$$\dot{\rho} = i[\rho, H_{\text{opt}}(t)] + \kappa \mathcal{D}[a]\rho + \gamma(\bar{n}_m + 1)\mathcal{D}[b]\rho + \gamma\bar{n}_m \mathcal{D}[b^\dagger]\rho, \quad (2)$$

where ρ is the density matrix of the optomechanical system, $\mathcal{D}[o]\rho = o\rho o^\dagger - (o^\dagger o\rho + \rho o^\dagger o)/2$ (for $o = a, a^\dagger, b, b^\dagger$) is the Lindblad superoperator [62], and $H_{\text{opt}}(t)$ is defined in Eq. (1). The parameters κ and γ are, respectively, the damping rates of the cavity field and the mechanical oscillation, and \bar{n}_m is the environmental thermal-excitation occupation of the mechanical resonator.

Considering the strong-driving case of the optomechanical cavity, then the dynamics of the system can be linearized. To this end, we adopt the displacement-transformation method to separate the semiclassical motion and quantum fluctuation. Concretely, we perform the displacement transformations $D_a(\alpha) = \exp(\alpha a^\dagger - \alpha^* a)$ and $D_b(\beta) = \exp(\beta b^\dagger - \beta^* b)$ for the density operator $\rho(t)$, namely,

$$\rho'(t) = D_a(\alpha)D_b(\beta)\rho(t)D_b^\dagger(\beta)D_a^\dagger(\alpha), \quad (3)$$

where $\rho'(t)$ represents the density operator in the displaced representation, $\alpha(t)$ and $\beta(t)$ are the displacement amplitudes of the cavity field and the mechanical resonator, respectively. By substituting $\rho(t) = D_b^\dagger(\beta)D_a^\dagger(\alpha)\rho'(t)D_a(\alpha)D_b(\beta)$ into Eq. (2) and setting the coefficients of the driving terms to be zero, we obtain the quantum master equation in the displaced representation as

$$\dot{\rho}' = i[\rho', H_{\text{dis}}(t)] + \kappa \mathcal{D}[a]\rho' + \gamma(\bar{n}_m + 1)\mathcal{D}[b]\rho' + \gamma\bar{n}_m \mathcal{D}[b^\dagger]\rho', \quad (4)$$

where $H_{\text{dis}}(t)$ is the Hamiltonian in the displaced representation, defined as

$$H_{\text{dis}}(t) = \Delta(t)a^\dagger a + \omega_m b^\dagger b - g_0 a^\dagger a (b + b^\dagger) + [G(t)a^\dagger + G^*(t)a](b + b^\dagger). \quad (5)$$

In Eq. (5), we introduce the linearized optomechanical-coupling strength $G(t) = g_0\alpha(t)$ and the normalized driving detuning $\Delta(t) = \Delta_c + g_0[\beta(t) + \beta^*(t)]$. The two displacement amplitudes $\alpha(t)$ and $\beta(t)$ are governed by the equations of motion,

$$\dot{\alpha}(t) = -\left[i\Delta(t) + \frac{\kappa}{2}\right]\alpha(t) + i\Omega(t)e^{-i\phi(t)}, \quad (6a)$$

$$\dot{\beta}(t) = -\left(i\omega_m + \frac{\gamma}{2}\right)\beta(t) - ig_0|\alpha(t)|^2. \quad (6b)$$

In the strong-driving case, $|\alpha(t)| \gg 1$, we can safely omit the g_0 term in Eq. (5), and obtain the linearized optomechanical Hamiltonian

$$H_{\text{lin}}(t) = \Delta(t)a^\dagger a + \omega_m b^\dagger b + [G(t)a^\dagger + G^*(t)a](b + b^\dagger), \quad (7)$$

Since both the linearized optomechanical-coupling strength $G(t)$ and the normalized driving detuning $\Delta(t)$ in Hamiltonian (7) depend on $\alpha(t)$ and $\beta(t)$, the dynamic evolution of the system can be controlled by adjusting the amplitude and phase of the pulsed driving, as shown by Eqs. (6a) and (6b).

The dynamic properties of the linearized optomechanical system are completely described by both the first- and second-order moments of the system operators. Using the relation $\partial_t \langle o_i o_j \rangle = \text{Tr}(\dot{\rho}' o_i o_j)$ for $o_i, o_j \in \{a, a^\dagger, b, b^\dagger\}$ and Eq. (4) under the replacement of $H_{\text{dis}}(t) \rightarrow H_{\text{lin}}(t)$, we obtain the equations of motion of all these second-order moments, which can be expressed as

$$\dot{\mathbf{X}}(t) = \mathbf{M}(t)\mathbf{X}(t) + \mathbf{N}(t), \quad (8)$$

where $\mathbf{X}(t) = (\langle a^\dagger a \rangle, \langle b^\dagger b \rangle, \langle a^\dagger b \rangle, \langle ab^\dagger \rangle, \langle a^\dagger a^\dagger \rangle, \langle a^\dagger b^\dagger \rangle, \langle b^\dagger b^\dagger \rangle, \langle aa \rangle, \langle ab \rangle, \langle bb \rangle)^T$ (“T” denotes the matrix transpose), $\mathbf{N}(t) = (0, \gamma\bar{n}_m, 0, 0, 0, ig_0\alpha^*, 0, 0, -ig_0\alpha, 0)^T$, and the coefficient matrix is introduced as $\mathbf{M}(t) = \begin{pmatrix} \mathbf{H} & \mathbf{I} \\ \mathbf{J} & \mathbf{K} \end{pmatrix}$, with

Algorithm. Mechanical squeezing generation

Input: A randomly smooth and continuous initial pulsed driving with amplitude Ω and phase ϕ .

Define: The loss function $\Delta X_b^2(\theta, T)$.

While $\Delta X_b^2(\theta, T) > \epsilon$ (ϵ is the expected value) **do**:

1. Perform the gradient-descent algorithm $\mathcal{Q}_{m+1} = \mathcal{Q}_m - \chi_{\mathcal{Q}} \{\delta[\Delta X_b^2(\theta, T)]/\delta \mathcal{Q}_m\}$ (\mathcal{Q} represents either Ω or ϕ , $\chi_{\mathcal{Q}}$ is the learning rate, and m indicates the iteration number) to iteratively minimize $\Delta X_b^2(\theta, T)$.

2. Optimize and update Ω and ϕ .

End While

Return: Variance $\Delta X_b^2(\theta, t)$, driving amplitude Ω , and phase ϕ .

$$\mathbf{H} = \begin{pmatrix} -\kappa & 0 & -ig_0\alpha & ig_0\alpha^* \\ 0 & -\gamma & ig_0\alpha & -ig_0\alpha^* \\ -ig_0\alpha^* & ig_0\alpha^* & K_1 & 0 \\ ig_0\alpha & -ig_0\alpha & 0 & K_1^* \end{pmatrix}, \quad (9a)$$

$$\mathbf{I} = \begin{pmatrix} 0 & -ig_0\alpha & 0 & 0 & ig_0\alpha^* & 0 \\ 0 & -ig_0\alpha & 0 & 0 & ig_0\alpha^* & 0 \\ -ig_0\alpha & 0 & 0 & 0 & 0 & ig_0\alpha^* \\ 0 & 0 & -ig_0\alpha & ig_0\alpha^* & 0 & 0 \end{pmatrix}, \quad (9b)$$

$$\mathbf{J} = \begin{pmatrix} 0 & 0 & 2ig_0\alpha^* & 0 \\ ig_0\alpha^* & ig_0\alpha^* & 0 & 0 \\ 0 & 0 & 0 & 2ig_0\alpha^* \\ 0 & 0 & 0 & -2ig_0\alpha \\ -ig_0\alpha & -ig_0\alpha & 0 & 0 \\ 0 & 0 & -2ig_0\alpha & 0 \end{pmatrix}, \quad (9c)$$

$$\mathbf{K} = \begin{pmatrix} K_2 & 2ig_0\alpha^* & 0 & 0 & 0 & 0 \\ ig_0\alpha & K_3 & ig_0\alpha^* & 0 & 0 & 0 \\ 0 & 2ig_0\alpha & K_4 & 0 & 0 & 0 \\ 0 & 0 & 0 & K_2^* & -2ig_0\alpha & 0 \\ 0 & 0 & 0 & -ig_0\alpha^* & K_3^* & 0 \\ 0 & 0 & 0 & 0 & -2ig_0\alpha^* & K_4^* \end{pmatrix}. \quad (9d)$$

In Eq. (9), we introduce

$$K_1 = i\Delta(t) - i\omega_m - \frac{1}{2}(\kappa + \gamma), \quad (10a)$$

$$K_2 = 2i\Delta(t) - \kappa, \quad (10b)$$

$$K_3 = i\Delta(t) + i\omega_m - \frac{1}{2}(\kappa + \gamma) \quad (10c)$$

$$K_4 = 2i\omega_m - \gamma. \quad (10d)$$

We point out that both the coefficient matrix $\mathbf{M}(t)$ and the inhomogeneous term $\mathbf{N}(t)$ are functions of the displacement amplitudes $\alpha(t)$ and $\beta(t)$, then the dynamic evolution of the second-order moments can be controlled via adjusting the pulsed driving.

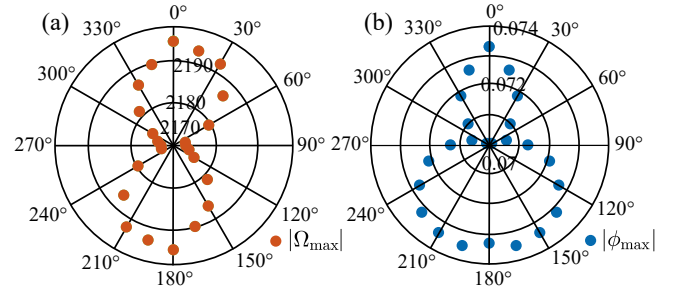


FIG. 1. Maximal absolute values of (a) the driving amplitude and (b) phase as functions of squeezing angle θ when the squeezing degree $\mathcal{S}_b = 1$. Here, the parameters used are $g_0/\omega_m = 4 \times 10^{-5}$, $\kappa/\omega_m = 0.2$, $\gamma/\omega_m = 2 \times 10^{-6}$, $T = 120\omega_m^{-1}$, $\bar{n}_m=100$, and $\Delta_c/\omega_m = 1$.

III. GENERATION OF MECHANICAL QUADRATURE SQUEEZING

To quantify the created mechanical squeezing, we introduce the quadrature operators $X_{o=a,b} = (o^\dagger + o)/\sqrt{2}$ and $Y_{o=a,b} = i(o^\dagger - o)/\sqrt{2}$ for the optical and mechanical modes. Then the transient correlation matrix can be introduced as

$$\mathbf{V}_{ij}(t) = \frac{1}{2}[\langle \mathbf{u}_i(t)\mathbf{u}_j(t) \rangle + \langle \mathbf{u}_j(t)\mathbf{u}_i(t) \rangle] + \langle \mathbf{u}_i(t) \rangle \langle \mathbf{u}_j(t) \rangle, \quad (11)$$

where $\mathbf{u}(t) = (X_a(t), Y_a(t), X_b(t), Y_b(t))^T$. In the present case, the expectation values $\langle \mathbf{u}_i(t) \rangle$ and $\langle \mathbf{u}_j(t) \rangle$ are zero and $\langle \mathbf{u}_i(t)\mathbf{u}_j(t) \rangle$ is a linear function of these second-order moments. To describe the quadrature squeezing, we further introduce the rotating-quadrature operator $X_b(\theta, t) \equiv X_b(t) \cos \theta + Y_b(t) \sin \theta$ (θ is the squeezing angle). The variance of the rotating-quadrature operator is given by

$$\Delta X_b^2(\theta, t) = \mathbf{V}_{33}(t) \cos^2 \theta + \mathbf{V}_{44}(t) \sin^2 \theta + \frac{1}{2}[\mathbf{V}_{34}(t) + \mathbf{V}_{43}(t)] \sin(2\theta). \quad (12)$$

Based on $[X_b(\theta, t), X_b(\theta + \pi, t)] = i$, we have $\Delta X_b^2(\theta, t) \Delta X_b^2(\theta + \pi, t) \geq 1/4$, then the quadrature squeezing of the mechanical mode occurs when $\Delta X_b^2(\theta, t) < 1/2$.

For squeezing-generation task, our goal is to reduce the variance $\Delta X_b^2(\theta, t)$ such that it is smaller than $1/2$. The control strategy of squeezing generation is summarized in **Algorithm**. Note that a variable learning rate method is adopted here to reduce the iteration number and to improve the efficiency. The detailed calculation of $\delta[\Delta X_b^2(\theta, T)]/\delta \mathcal{Q}_m$ is shown in Appendix.

The mechanical quadrature squeezing can be well quantized by the squeezing degree [38]

$$\mathcal{S}_b = -10 \log_{10} \frac{\Delta X_b^2(\theta, t)}{\Delta X_b^2(\theta)|_{\text{zpf}}}. \quad (13)$$

A positive squeezing degree, $\mathcal{S}_b > 0$, implies that the quadrature operator of the mechanical mode is squeezed

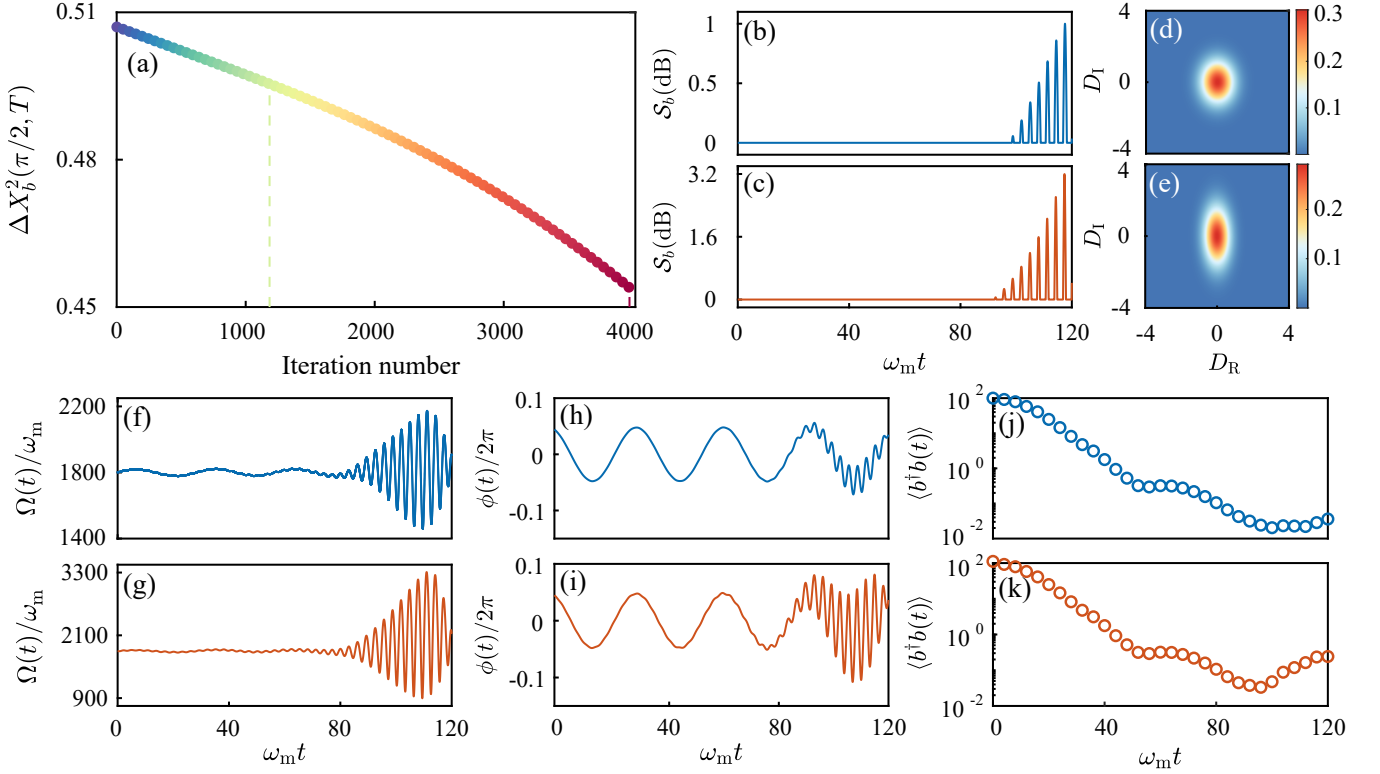


FIG. 2. (a) The loss function $\Delta X_b^2(\theta = \pi/2, T)$ as a function of the iteration number. The squeezing degree S_b versus the scaled evolution time $\omega_m t$ under different target squeezing degrees: (b) $S_b = 1$ and (c) $S_b = 3.2$. (d, e) The Wigner functions of the generated states for the mechanical mode corresponding to the maximal squeezing in panels (b, c). (f, g) The scaled driving amplitude $\Omega(t)/\omega_m$, (h, i) phase $\phi(t)/2\pi$, and (j, k) mean phonon number $\langle b^\dagger b \rangle$ as functions of the scaled evolution time $\omega_m t$ corresponding to panels (b, c). Other parameters used are the same as those given in Fig. 1.

along the angle θ . For studying the rotating-quadrature squeezing, we need to investigate the dependence of the squeezing on the angle θ . Concretely, we use the gradient-descent algorithm to obtain the waveforms of the driving amplitude and phase corresponding to $S_b = 1$ at different values of θ . The results shown in Fig. 1(a) indicate that the smallest (largest) driving amplitude appears at the squeezing angle 90° (0°) related to $S_b = 1$. Similarly, the minimal and maximal driving phases appear at 65° and 165° , respectively, and the angle has little effect on the phase [as shown in Fig. 1(b)]. Therefore, we take the squeezing angle $\theta = 90^\circ$ (corresponding to minimal driving amplitude) in our following discussions.

We display in Fig. 2(a) the loss function $\Delta X_b^2(\pi/2, T)$ as a function of the iteration number to verify the efficiency of the gradient-descent algorithm. Here, we can see that the loss function $\Delta X_b^2(\pi/2, T)$ decreases gradually as the iteration number increases. The transient mechanical squeezing degrees 1 dB and 3.2 dB are obtained at the iteration numbers 1185 and 4000, respectively. The corresponding dynamic evolution of the squeezing degree S_b are shown in Figs. 2(b) and 2(c). It shows that there are no mechanical squeezing for a long duration of time firstly, and then oscillatingly increase to the target value in a short period of time. In particular, the squeez-

ing degree $S_b = 3.2$ breaks the 3 dB steady-state limit [Fig. 2(c)], and stronger squeezings can be realized as the iteration number increases. Note that we consider the transient squeezing here rather than steady-state squeezing. Therefore, our results are not conflicting with the 3 dB steady-state squeezing limit, which is determined by the dynamic stability.

To confirm the mechanical squeezing in phase space, we introduce the Wigner function of the mechanical mode, defined as [63]

$$W(\mathbf{D}) = \frac{1}{2\pi\sqrt{\text{Det}[\mathbf{V}_b]}} \exp\left\{-\frac{1}{2}\mathbf{D}^T \mathbf{V}_b \mathbf{D}\right\}, \quad (14)$$

where $\mathbf{D} = (D_R, D_I)^T$ represents the two-dimensional vector, and \mathbf{V}_b is the covariance matrix for the mechanical mode. The Wigner functions corresponding to 1 dB and 3.2 dB squeezing are shown in Figs. 2(d) and 2(e). We can see that the squeezing appears along the $\pi/2$ -axis (corresponding to the squeezing angle $\theta = \pi/2$), and the larger the squeezing degree, the stronger the quadrature squeezing.

In Figs. 2(f) and 2(g), we show the time-dependent driving amplitudes, which are required to achieve the squeezing degrees $S_b = 1$ dB and 3.2 dB, respectively [64]. We can see that a larger driving amplitude is required to

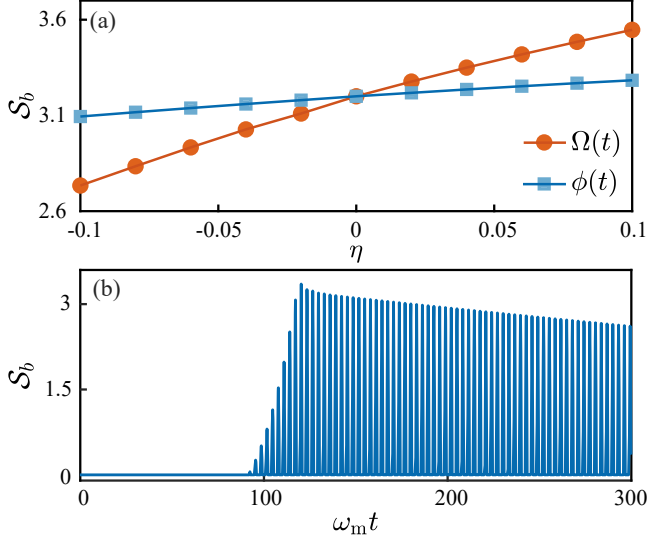


FIG. 3. (a) The influence of the driving amplitude and phase deviations on the squeezing generation at $T = 120\omega_m^{-1}$ related to $S_b = 3.2$. (b) The dynamic evolution of the squeezing degree S_b after removing the pulsed driving in Fig. 2(c). Other parameters used are consistent with those given in Fig. 1.

realize a stronger squeezing. In addition, for a larger mechanical squeezing degree, the driving phase oscillation becomes more intense, as shown in Figs. 2(h) and 2(i). We also investigate the dependence of the mean phonon number $\langle b^\dagger b \rangle$ (in the displaced representation, associated with the quantum fluctuation) as a function of the scaled time $\omega_m t$ in Figs. 2(j) and 2(k). We observe that $\langle b^\dagger b \rangle$ decreases from one hundred to less than one for both $S_b = 1$ dB and 3.2 dB. Note that these results can be well understood by examining the statistical properties for the squeezed vacuum state. For a single-mode squeezed vacuum state, the mean phonon number is $\sinh^2 r$, which is a function of the squeezing amplitude r . Further, the covariance of the mechanical rotating-quadrature operator in the squeezing-vacuum state is $(2\sinh^2 r + 1 - 2\sinh r \cosh r \cos \varphi)/2$, (φ is the difference between the rotation angle and the squeezing angle). Considering $\varphi = 0$, then we can numerically verify that the squeezing amplitude corresponding to the squeezing degree $S_b = 3$ is $r = 0.347$, and the mean phonon number is 0.125. This indicates that the mechanical squeezing exists even if the mechanical resonator is cooled near the ground state.

To explore the influence of the deviations in $\Omega(t)$ and $\phi(t)$ on mechanical quadrature squeezing, we introduce the relative deviation η , defined as $\eta = (Q_r - Q_t)/Q_t$. Here Q represents either Ω or ϕ , Q_r and Q_t stand for the realistically used parameters and the learned theoretical parameters, respectively. In Fig. 3(a), we plot the squeezing degree S_b as a function of η . Here, we see that for the relative deviation $\eta \in [-0.1, 0.1]$, the S_b is an increasing function of η for both the driving amplitude and phase.

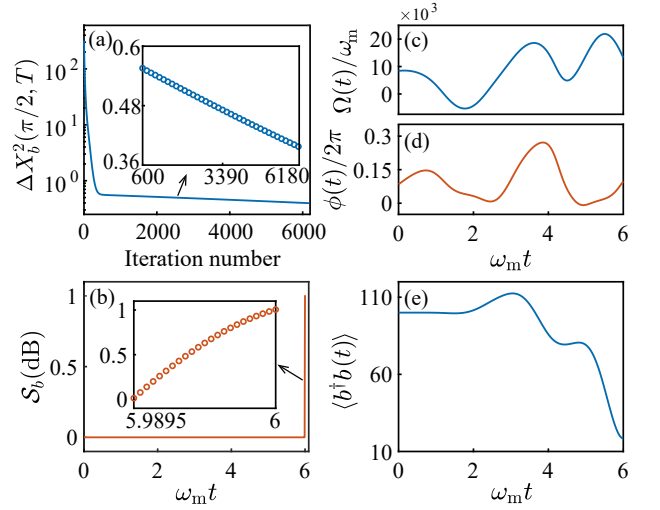


FIG. 4. (a) The loss function $\Delta X_b^2(\pi/2, T)$ as a function of the iteration number under $T = 6\omega_m^{-1}$. The inset shows the local magnification of the loss function over the iteration interval [600, 6180]. (b) Evolution of the squeezing degree S_b in one mechanical oscillation period. The inset shows the evolution of S_b over time duration [5.9895, 6]. (c) The driving amplitude $\Omega(t)/\omega_m$ and (d) phase $\phi(t)/2\pi$ versus the scaled evolution time $\omega_m t$ after the last iteration ($m = 6180$) under $T = 6\omega_m^{-1}$. (e) The mean phonon number $\langle b^\dagger b \rangle$ as a function of the scaled evolution time $\omega_m t$ corresponding to panel (b). Other parameters used are the same as those given in Fig. 1.

In addition, the squeezing is more sensitive to amplitude deviation than phase deviation. In Fig. 3(b), we further investigate the influence of the environment on the squeezing generation once the pulsed driving is removed at $T = 120\omega_m^{-1}$. The S_b will experience a slightly decrease from 3.2 to 2.51 during the period from $\omega_m t = 120$ to 300, indicating that the squeezing has a good robustness.

Ultrafast generation of mechanical squeezing is a desired task from the viewpoint of transient evolution. Below, we investigate the generation of mechanical squeezing within one mechanical oscillation period. Figure 4(a) shows the loss function $\Delta X_b^2(\pi/2, T = 6\omega_m^{-1})$ versus the iteration number related to $S_b = 1$. Here we can see that the $\Delta X_b^2(\pi/2, T = 6\omega_m^{-1})$ gradually decreases from the initial value 319 to 0.397 as the iteration number increases, verifying the validity of the gradient-descent algorithm. The dynamic evolution of the squeezing degree S_b after the last iteration ($m = 6180$) is shown in Fig. 4(b). We see that the squeezing occurs in the last extremely short duration due to the harsh time condition, but it is still continuous, as shown in the inset of Fig. 4(b). The results in Figs. 4(c) and 4(d) indicate that a large driving amplitude is required to achieve $S_b = 1$ within one mechanical oscillation period and the phase has no distinct signature. We also exhibit in Fig. 4(e) the mean phonon number $\langle b^\dagger b \rangle$ versus the scaled evolution time at this time. Here we see that $\langle b^\dagger b \rangle$ will be larger than the initial value due to the larger driving amplitude, and

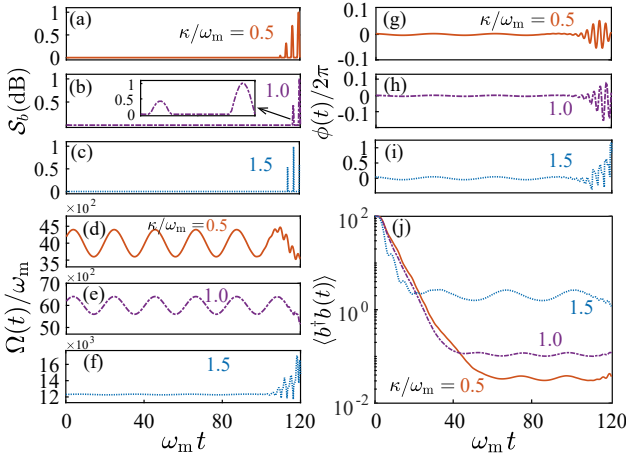


FIG. 5. (a-c) The squeezing degree \mathcal{S}_b versus the scaled evolution time $\omega_m t$ under different sideband parameters $\kappa/\omega_m = 0.5, 1.0$, and 1.5 . The inset in panel (b) exhibits the evolution of \mathcal{S}_b for the time durations from 115.6 to 120. (d-f) Evolution of driving amplitude and (g-i) phase corresponding to panels (a-c). (j) The dynamic evolution of the mean phonon number under different sideband-resolution parameters in panels (a-c). Other parameters are consistent with those given in Fig. 1.

then goes to a cooled state with dozens of mean phonons. This indicates that the creation of mechanical squeezing does not necessarily require the ground-state cooling of the mechanical resonator.

We also investigate the influence of the sideband-resolution parameter on the squeezing generation. In Figs. 5(a-c), we plot the squeezing degree \mathcal{S}_b versus the scaled evolution time $\omega_m t$ corresponding to different sideband-resolution parameters $\kappa/\omega_m = 0.5, 1.0$, and 1.5 . We show the driving amplitude and phase as functions of $\omega_m t$ for different sideband-resolution parameters in Figs. 5(d-f) and Figs. 5(g-i). To maintain $\mathcal{S}_b = 1$, a larger driving amplitude is needed for a larger value of κ/ω_m , and the phase oscillation becomes more severe for a larger κ/ω_m . The corresponding dynamic evolution of the mean phonon number $\langle b^\dagger b \rangle$ is shown in Fig. 5(j). Here we can see that the mechanical resonator is cooled from the initial one hundred phonons to a few phonons. The better the sideband-resolution parameter is selected, the deeper cooling of the mechanical resonator. Note that a large κ/ω_m will result in fast photon dissipation within the cavity, thereby affecting the optomechanical interaction and leading to the failure of squeezing generation.

IV. DISCUSSIONS AND CONCLUSION

In this section, we present some discussions on the physical mechanism and experimental implementation of this scheme and conclude this work. The mechanical squeezing generation can be understood by analyzing the

variance of the mechanical rotating-quadrature operator $\Delta X_b^2(\theta, t) = \mathbf{V}_{33}(t) \cos^2 \theta + \mathbf{V}_{44}(t) \sin^2 \theta + \frac{1}{2}[\mathbf{V}_{34}(t) + \mathbf{V}_{43}(t)] \sin(2\theta)$. To be more clear, we re-express the variance as

$$\Delta X_b^2(\theta, t) = \frac{1}{2} + \langle b^\dagger b \rangle + \text{Re}[\langle b^\dagger b^\dagger \rangle] \cos(2\theta) - 2\text{Im}[\langle b^\dagger b^\dagger \rangle] \sin(2\theta). \quad (15)$$

Since the mechanical squeezing occurs when $\Delta X_b^2(\theta, t) < 1/2$, our goal is to realize $\langle b^\dagger b \rangle + \text{Re}[\langle b^\dagger b^\dagger \rangle] \cos(2\theta) - 2\text{Im}[\langle b^\dagger b^\dagger \rangle] \sin(2\theta) < 0$, which is feasible because the second-order moment $\langle b^\dagger b^\dagger \rangle$ could be a complex number. Meanwhile, the value of $\langle b^\dagger b \rangle$ must be a positive number, and then the reduction of $\langle b^\dagger b \rangle$ is beneficial to the squeezing generation, which explains why the mechanical resonator is cooled [Figs. 2(j), 2(k), 4(e), and 5(j)]. In addition, under the rotating-wave approximation, we have two sets of equations governing all these second-order moments. The first set includes $\langle a^\dagger a \rangle$, $\langle b^\dagger b \rangle$, $\langle a^\dagger b \rangle$, and $\langle ab^\dagger \rangle$, while the second set includes $\langle a^\dagger a^\dagger \rangle$, $\langle aa \rangle$, $\langle b^\dagger b^\dagger \rangle$, $\langle bb \rangle$, $\langle a^\dagger b^\dagger \rangle$, and $\langle ab \rangle$. Initially, with the condition $\mathbf{X}(0) = [0, \bar{n}_m, 0, 0, 0, 0, 0, 0, 0, 0]^T$, the value of $\langle b^\dagger b^\dagger \rangle$ remains constantly zero, making mechanical squeezing unattainable regardless of how we optimize the driving field. In the presence of the counter-rotating terms, the equations of motion for these ten second-order moments are coupled to each other. Consequently, $\langle b^\dagger b^\dagger \rangle$ is no longer zero. In this case, we can obtain $\langle b^\dagger b \rangle + \text{Re}[\langle b^\dagger b^\dagger \rangle] \cos(2\theta) - 2\text{Im}[\langle b^\dagger b^\dagger \rangle] \sin(2\theta) < 0$ via optimizing the pulsed driving. These analyses indicate that the counter-rotating terms play a crucial role in the generation of mechanical quadrature squeezing.

We now present some discussions on the experimental feasibility of this scheme. The system under considerations is a general optomechanical system, which has been implemented in various optomechanical platforms, such as optical microresonators [65–67], electromechanical systems [68–70], photonic crystal nanobeams [5, 71, 72], and Fabry-Pérot cavities [73], in which the cavities can be driven by tunable pulsed fields. We considered the linearized optomechanical interaction, which has been widely demonstrated in cavity optomechanical systems. Moreover, we use the experimentally accessible parameters in our numerical simulations. Concretely, the used parameters are $g_0/\omega_m = 4 \times 10^{-5}$, $\kappa/\omega_m = 0.2$, and $\gamma/\omega_m = 2 \times 10^{-6}$, which have been reported in experiments [67]. In addition, the pulsed driving amplitude and phase used to generate squeezing are moderate in size and continuous and smooth in shape, which confirm the experimental realization of the pulsed driving.

In conclusion, we have presented a scheme for generating mechanical quadrature squeezing in a typical optomechanical system via gradient-descent algorithm. The generated mechanical squeezing can exceed the 3 dB steady-state limit and ultrafast squeezing preparation within one mechanical oscillation period can be realized. The optimal driving amplitude and phase corresponding to these generated squeezings have been presented. Our scheme

will pave the way for exploiting optimal quantum control in quantum optics and quantum information science.

ACKNOWLEDGMENTS

The authors thank Dr. Ye-Xiong Zeng and Dr. Yue-Hui Zhou for helpful discussions. J.-Q.L. was sup-

ported in part by National Natural Science Foundation of China (Grants No. 12175061, No. 12247105, and No. 11935006), the Science and Technology Innovation Program of Hunan Province (Grant No. 2021RC4029), and Hunan Provincial Major Science and Technology Program (Grant No. 2023ZJ1010).

Appendix: Derivation of the variation $\delta[\Delta X_b^2(\theta, T)]/\delta \mathcal{Q}_m$

For generation of mechanical quadrature squeezing, we need to minimize the loss function $\Delta X_b^2(\theta, T)$. In this Appendix, we will clarify in detail how to achieve this goal using the gradient-descent algorithm. The mathematical expression of the gradient-descent algorithm for mechanical squeezing generation is

$$\mathcal{Q}_{m+1} = \mathcal{Q}_m - \chi_{\mathcal{Q}} \frac{\delta[\Delta X_b^2(\theta, T)]}{\delta \mathcal{Q}_m}, \quad (\text{A.1})$$

where \mathcal{Q} could be either Ω or ϕ , m is the iteration number, and $\chi_{\mathcal{Q}}$ is the learning rate. To calculate Eq. (A.1), we need to calculate the variation of $\Delta X_b^2(\theta, T)$ with respect to the pulse amplitude $\Omega(s)$ and phase $\phi(s)$. Based on Eq. (12), we can obtain the result

$$\frac{\delta \Delta X_b^2(\theta, T)}{\delta \mathcal{Q}(s)} = \frac{\delta V_{33}(T)}{\delta \mathcal{Q}(s)} \cos^2 \theta + \frac{\delta V_{44}(T)}{\delta \mathcal{Q}(s)} \sin^2 \theta + \left[\frac{\delta V_{34}(T)}{\delta \mathcal{Q}(s)} + \frac{\delta V_{43}(T)}{\delta \mathcal{Q}(s)} \right] \sin(2\theta). \quad (\text{A.2})$$

According to Eq. (A.2), we can further calculate the results of $\delta V_{33}(T)/\delta \mathcal{Q}(s)$, $\delta V_{44}(T)/\delta \mathcal{Q}(s)$, $\delta V_{34}(T)/\delta \mathcal{Q}(s)$, and $\delta V_{43}(T)/\delta \mathcal{Q}(s)$. The variation of the covariance-matrix elements with respect to the pulse amplitude $\Omega(t)$ and phase $\phi(t)$ can be expressed as a linear combination of the variation of these second-order moments with respect to the driving amplitude $\Omega(t)$ and phase $\phi(t)$,

$$\frac{\delta V_{11}(T)}{\delta \mathcal{Q}(s)} = \frac{1}{2} \frac{\delta \langle a^\dagger a^\dagger(T) \rangle}{\delta \mathcal{Q}(s)} + \frac{\delta \langle a^\dagger a(T) \rangle}{\delta \mathcal{Q}(s)} + \frac{1}{2} \frac{\delta \langle aa(T) \rangle}{\delta \mathcal{Q}(s)}, \quad (\text{A.3a})$$

$$\frac{\delta V_{12}(T)}{\delta \mathcal{Q}(s)} = \frac{i}{2} \frac{\delta \langle a^\dagger a^\dagger(T) \rangle}{\delta \mathcal{Q}(s)} - \frac{i}{2} \frac{\delta \langle aa(T) \rangle}{\delta \mathcal{Q}(s)}, \quad (\text{A.3b})$$

$$\frac{\delta V_{13}(T)}{\delta \mathcal{Q}(s)} = \frac{1}{2} \frac{\delta \langle a^\dagger b^\dagger(T) \rangle}{\delta \mathcal{Q}(s)} + \frac{1}{2} \frac{\delta \langle a^\dagger b(T) \rangle}{\delta \mathcal{Q}(s)} + \frac{1}{2} \frac{\delta \langle ab^\dagger(T) \rangle}{\delta \mathcal{Q}(s)} + \frac{1}{2} \frac{\delta \langle ab(T) \rangle}{\delta \mathcal{Q}(s)}, \quad (\text{A.3c})$$

$$\frac{\delta V_{14}(T)}{\delta \mathcal{Q}(s)} = \frac{i}{2} \frac{\delta \langle a^\dagger b^\dagger(T) \rangle}{\delta \mathcal{Q}(s)} - \frac{i}{2} \frac{\delta \langle a^\dagger b(T) \rangle}{\delta \mathcal{Q}(s)} + \frac{i}{2} \frac{\delta \langle ab^\dagger(T) \rangle}{\delta \mathcal{Q}(s)} - \frac{i}{2} \frac{\delta \langle ab(T) \rangle}{\delta \mathcal{Q}(s)}, \quad (\text{A.3d})$$

$$\frac{\delta V_{22}(T)}{\delta \mathcal{Q}(s)} = -\frac{1}{2} \frac{\delta \langle a^\dagger a^\dagger(T) \rangle}{\delta \mathcal{Q}(s)} + \frac{\delta \langle a^\dagger a(T) \rangle}{\delta \mathcal{Q}(s)} - \frac{1}{2} \frac{\delta \langle aa(T) \rangle}{\delta \mathcal{Q}(s)}, \quad (\text{A.3e})$$

$$\frac{\delta V_{23}(T)}{\delta \mathcal{Q}(s)} = \frac{i}{2} \frac{\delta \langle a^\dagger b^\dagger(T) \rangle}{\delta \mathcal{Q}(s)} + \frac{i}{2} \frac{\delta \langle a^\dagger b(T) \rangle}{\delta \mathcal{Q}(s)} - \frac{i}{2} \frac{\delta \langle ab^\dagger(T) \rangle}{\delta \mathcal{Q}(s)} - \frac{i}{2} \frac{\delta \langle ab(T) \rangle}{\delta \mathcal{Q}(s)}, \quad (\text{A.3f})$$

$$\frac{\delta V_{24}(T)}{\delta \mathcal{Q}(s)} = -\frac{1}{2} \frac{\delta \langle a^\dagger b^\dagger(T) \rangle}{\delta \mathcal{Q}(s)} + \frac{1}{2} \frac{\delta \langle a^\dagger b(T) \rangle}{\delta \mathcal{Q}(s)} + \frac{1}{2} \frac{\delta \langle ab^\dagger(T) \rangle}{\delta \mathcal{Q}(s)} - \frac{1}{2} \frac{\delta \langle ab(T) \rangle}{\delta \mathcal{Q}(s)}, \quad (\text{A.3g})$$

$$\frac{\delta V_{33}(T)}{\delta \mathcal{Q}(s)} = \frac{1}{2} \frac{\delta \langle b^\dagger b^\dagger(T) \rangle}{\delta \mathcal{Q}(s)} + \frac{\delta \langle b^\dagger b(T) \rangle}{\delta \mathcal{Q}(s)} + \frac{1}{2} \frac{\delta \langle bb(T) \rangle}{\delta \mathcal{Q}(s)}, \quad (\text{A.3h})$$

$$\frac{\delta V_{34}(T)}{\delta \mathcal{Q}(s)} = \frac{i}{2} \frac{\delta \langle b^\dagger b^\dagger(T) \rangle}{\delta \mathcal{Q}(s)} - \frac{i}{2} \frac{\delta \langle bb(T) \rangle}{\delta \mathcal{Q}(s)}, \quad (\text{A.3i})$$

$$\frac{\delta V_{44}(T)}{\delta \mathcal{Q}(s)} = -\frac{1}{2} \frac{\delta \langle b^\dagger b^\dagger(T) \rangle}{\delta \mathcal{Q}(s)} + \frac{\delta \langle b^\dagger b(T) \rangle}{\delta \mathcal{Q}(s)} - \frac{1}{2} \frac{\delta \langle bb(T) \rangle}{\delta \mathcal{Q}(s)}. \quad (\text{A.3j})$$

The variation for other covariance-matrix elements can be obtained based on the Hermitian conjugate relations.

It can be seen from Eq. (A.3) that, to obtain the result in Eq. (A.2), we need to further calculate the variations of these second-order moments with respect to $\Omega(t)$ and $\phi(t)$. This can be achieved by taking the variation with respect to $\Omega(s)$ and $\phi(s)$ on both sides of Eq. (8), namely,

$$\frac{\delta \dot{\mathbf{X}}(t)}{\delta \mathcal{Q}(s)} = \mathbf{M}(t) \frac{\delta \mathbf{X}(t)}{\delta \mathcal{Q}(s)} + \frac{\delta \mathbf{M}(t)}{\delta \mathcal{Q}(s)} \mathbf{X}(t) + \frac{\delta \mathbf{N}(t)}{\delta \mathcal{Q}(s)}. \quad (\text{A.4})$$

Since $\mathcal{Q}(s)$ is a function of s , $\delta \dot{\mathbf{X}}(t)/\delta \mathcal{Q}(s)$ in Eq. (A.4) can be expressed as $\frac{d}{dt} \frac{\delta \mathbf{X}(t)}{\delta \mathcal{Q}(s)}$ [74]. Under the initial condition $\delta \mathbf{X}(0)/\delta \mathcal{Q}(s) = [0, \dots, 0]_{10 \times 1}^T$, the solution of Eq. (A.4) at the target time T can be obtained as

$$\begin{aligned} \frac{\delta \mathbf{X}(T)}{\delta \mathcal{Q}(s)} &= \mathbf{U}(T) \frac{\delta \mathbf{X}(0)}{\delta \mathcal{Q}(s)} + \mathbf{U}(T) \int_0^T d\tau \mathbf{U}^{-1}(\tau) \left[\frac{\delta \mathbf{M}(\tau)}{\delta \mathcal{Q}(s)} \mathbf{X}(\tau) + \frac{\delta \mathbf{N}(\tau)}{\delta \mathcal{Q}(s)} \right] \\ &= \mathbf{U}(T) \int_0^T d\tau \mathbf{U}^{-1}(\tau) \left[\frac{\delta \mathbf{M}(\tau)}{\delta \mathcal{Q}(\tau)} \frac{\delta \mathcal{Q}(\tau)}{\delta \mathcal{Q}(s)} \mathbf{X}(\tau) + \frac{\delta \mathbf{N}(\tau)}{\delta \mathcal{Q}(\tau)} \frac{\delta \mathcal{Q}(\tau)}{\delta \mathcal{Q}(s)} \right] \\ &= \mathbf{U}(T) \mathbf{U}^{-1}(s) \left[\frac{\delta \mathbf{M}(s)}{\delta \mathcal{Q}(s)} \mathbf{X}(s) + \frac{\delta \mathbf{N}(s)}{\delta \mathcal{Q}(s)} \right], \end{aligned} \quad (\text{A.5})$$

where $\mathbf{U}(t)$ satisfies $\dot{\mathbf{U}}(t) = \mathbf{M}(t)\mathbf{U}(t)$ with the initial value $\mathbf{U}(0) = I$.

To know the explicit expressions for $\delta \mathbf{M}(s)/\delta \mathcal{Q}(s)$ and $\delta \mathbf{N}(s)/\delta \mathcal{Q}(s)$ in Eq. (A.5), we need to obtain the values of $\delta \alpha(s)/\delta \mathcal{Q}(s)$, $\delta \beta(s)/\delta \mathcal{Q}(s)$, and their Hermitian conjugate. Taking the variation with respect to $\mathcal{Q}(s)$ on both sides of Eqs. (6a) and (6b) as well as their Hermitian conjugate equations, we have

$$\dot{\mathbf{A}}(t) = \mathbf{W}(t)\mathbf{A}(t) + \mathbf{Q}(t), \quad (\text{A.6})$$

where

$$\mathbf{A}(t) = \left(\frac{\delta \alpha(t)}{\delta \mathcal{Q}(s)}, \frac{\delta \beta(t)}{\delta \mathcal{Q}(s)}, \frac{\delta \alpha^*(t)}{\delta \mathcal{Q}(s)}, \frac{\delta \beta^*(t)}{\delta \mathcal{Q}(s)} \right)^T, \quad (\text{A.7})$$

$$\mathbf{W}(t) = \begin{pmatrix} -i\Delta(t) - \frac{\kappa}{2} & 0 & -ig_0\alpha & -ig_0\alpha \\ -ig_0\alpha^* & -ig_0\alpha & -i\omega_m - \frac{\gamma}{2} & 0 \\ 0 & i\Delta(t) - \frac{\kappa}{2} & ig_0\alpha^* & ig_0\alpha^* \\ ig_0\alpha^* & ig_0\alpha & 0 & i\omega_m - \frac{\gamma}{2} \end{pmatrix}, \quad (\text{A.8})$$

and

$$\mathbf{Q}(t) = \begin{pmatrix} i \frac{\delta \Omega(t)}{\delta \mathcal{Q}(s)} e^{-i\phi(t)} + i\Omega(t) \frac{\delta[e^{-i\phi(t)}]}{\delta \mathcal{Q}(s)} \\ 0 \\ -i \frac{\delta \Omega(t)}{\delta \mathcal{Q}(s)} e^{i\phi(t)} - i\Omega(t) \frac{\delta[e^{i\phi(t)}]}{\delta \mathcal{Q}(s)} \\ 0 \end{pmatrix}. \quad (\text{A.9})$$

The solution to Eq. (A.6) can be expressed as

$$\mathbf{A}(t) = \Lambda(t)\mathbf{A}(0) + \Lambda(t) \int_0^t \Lambda^{-1}(\tau) \mathbf{Q}(\tau) d\tau, \quad (\text{A.10})$$

where $\mathbf{A}(0) = [0, 0, 0, 0]^T$ and $\Lambda(t)$ satisfies the equation $\dot{\Lambda}(t) = \mathbf{W}(t)\Lambda(t)$ with the initial value $\Lambda(0) = I$. Then, we have

$$\left(\frac{\delta \alpha(s)}{\delta \Omega(s)}, \frac{\delta \beta(s)}{\delta \Omega(s)}, \frac{\delta \alpha^*(s)}{\delta \Omega(s)}, \frac{\delta \beta^*(s)}{\delta \Omega(s)} \right)^T = \left(\frac{1}{2} i e^{-i\phi(s)}, 0, -\frac{1}{2} i e^{i\phi(s)}, 0 \right)^T, \quad (\text{A.11a})$$

$$\left(\frac{\delta \alpha(s)}{\delta \phi(s)}, \frac{\delta \beta(s)}{\delta \phi(s)}, \frac{\delta \alpha^*(s)}{\delta \phi(s)}, \frac{\delta \beta^*(s)}{\delta \phi(s)} \right)^T = \left(\frac{1}{2} \Omega(s) e^{-i\phi(s)}, 0, \frac{1}{2} \Omega(s) e^{i\phi(s)}, 0 \right)^T. \quad (\text{A.11b})$$

Thus, we obtain the variation of the displacement amplitudes $\alpha(s)$ and $\beta(s)$ with respect to the driving amplitude $\Omega(s)$ and phase $\phi(s)$, respectively. Based on the value of $\delta[\Delta X_b^2(\theta, T)]/\delta Q(s)$, we can further perform the gradient-descent algorithm until a satisfactory value of the loss function $\Delta X_b^2(\theta, T)$ is obtained.

-
- [1] M. Aspelmeyer, T. J. Kippenberg, and F. Marquardt, Cavity optomechanics, *Rev. Mod. Phys.* **86**, 1391 (2014).
 - [2] I. Wilson-Rae, N. Nooshi, W. Zwerger, and T. J. Kippenberg, Theory of Ground State Cooling of a Mechanical Oscillator Using Dynamical Backaction, *Phys. Rev. Lett.* **99**, 093901 (2007).
 - [3] F. Marquardt, J. P. Chen, A. A. Clerk, and S. M. Girvin, Quantum Theory of Cavity-Assisted Sideband Cooling of Mechanical Motion, *Phys. Rev. Lett.* **99**, 093902 (2007).
 - [4] J. Chan, T. P. M. Alegre, A. H. Safavi-Naeini, J. T. Hill, A. Krause, S. Gröblacher, M. Aspelmeyer, and O. Painter, Laser cooling of a nanomechanical oscillator into its quantum ground state, *Nature (London)* **478**, 89 (2011).
 - [5] J. D. Teufel, T. Donner, D. Li, J. W. Harlow, M. S. Allman, K. Cicak, A. J. Sirois, J. D. Whittaker, K. W. Lehnert, and R. W. Simmonds, Sideband cooling of micromechanical motion to the quantum ground state, *Nature (London)* **475**, 359 (2011).
 - [6] D. Vitali, S. Gigan, A. Ferreira, H. R. Böhm, P. Tombesi, A. Guerreiro, V. Vedral, A. Zeilinger, and M. Aspelmeyer, Optomechanical Entanglement between a Movable Mirror and a Cavity Field, *Phys. Rev. Lett.* **98**, 030405 (2007).
 - [7] T. A. Palomaki, J. D. Teufel, R. W. Simmonds, and K. W. Lehnert, Entangling mechanical motion with microwave fields, *Science* **342**, 710 (2013).
 - [8] R. Riedinger, S. Hong, R. A. Norte, J. A. Slater, J. Shang, A. G. Krause, V. Anant, M. Aspelmeyer, and S. Gröblacher, Non-classical correlations between single photons and phonons from a mechanical oscillator, *Nature (London)* **530**, 313 (2016).
 - [9] Y.-F. Jiao, S.-D. Zhang, Y.-L. Zhang, A. Miranowicz, L.-M. Kuang, and H. Jing, Nonreciprocal Optomechanical Entanglement against Backscattering Losses, *Phys. Rev. Lett.* **125**, 143605 (2020).
 - [10] H. Yu, L. McCuller, M. Tse, N. Kijbunchoo, L. Barsotti, N. Mavalvala, and L. S. Collaboration, Quantum correlations between light and the kilogram-mass mirrors of LIGO, *Nature (London)* **583**, 43 (2020).
 - [11] D.-G. Lai, J.-Q. Liao, A. Miranowicz, and F. Nori, Noise Tolerant Optomechanical Entanglement via Synthetic Magnetism, *Phys. Rev. Lett.* **129**, 063602 (2022).
 - [12] S. Bose, K. Jacobs, and P. L. Knight, Preparation of nonclassical states in cavities with a moving mirror, *Phys. Rev. A* **56**, 4175 (1997).
 - [13] W. Marshall, C. Simon, R. Penrose, and D. Bouwmeester, Towards Quantum Superpositions of a Mirror, *Phys. Rev. Lett.* **91**, 130401 (2003).
 - [14] J.-Q. Liao and L. Tian, Macroscopic Quantum Superposition in Cavity Optomechanics, *Phys. Rev. Lett.* **116**, 163602 (2016).
 - [15] J.-Q. Liao, J.-F. Huang, L. Tian, L.-Ma. Kuang, and C.-P. Sun, Generalized ultrastrong optomechanical-like coupling, *Phys. Rev. A* **101**, 063802 (2020).
 - [16] C. Fabre, M. Pinard, S. Bourzeix, A. Heidmann, E. Giacobino, and S. Reynaud, Quantum-noise reduction using a cavity with a movable mirror, *Phys. Rev. A* **49**, 1337 (1994).
 - [17] S. Mancini and P. Tombesi, *Phys. Rev. A* **49**, 4055 (1994).
 - [18] D. W. C. Brooks, T. Botter, S. Schreppler, T. P. Purdy, N. Brahms, and D. M. Stamper-Kurn, Non-classical light generated by quantum-noise-driven cavity optomechanics, *Nature (London)* **488**, 476 (2012).
 - [19] T. P. Purdy, P.-L. Yu, R. W. Peterson, N. S. Kampel, and C. A. Regal, Strong Optomechanical Squeezing of Light, *Phys. Rev. X* **3**, 031012 (2013).
 - [20] A. H. Safavi-Naeini, S. Gröblacher, J. T. Hill, J. Chan, M. Aspelmeyer, and O. Painter, Squeezed light from a silicon micromechanical resonator, *Nature (London)* **500**, 185 (2013).
 - [21] Kenan Qu and G. S. Agarwal, Strong squeezing via phonon mediated spontaneous generation of photon pairs, *New J. Phys.* **16**, 113004 (2014).
 - [22] M. J. Woolley, A. C. Doherty, G. J. Milburn, and K. C. Schwab, *Phys. Rev. A* **78**, 062303 (2008).
 - [23] J. Teufel, T. Donner, M. Castellanos-Beltran, J. Harlow, and K. Lehnert, Nanomechanical motion measured with an imprecision below that at the standard quantum limit, *Nat. Nanotechnol.* **4**, 820 (2009).
 - [24] A. Nunnenkamp, K. Børkje, J. Harris, and S. Girvin, Cooling and squeezing via quadratic optomechanical coupling, *Phys. Rev. A* **82**, 021806(R) (2010).
 - [25] J.-Q. Liao and C. K. Law, Parametric generation of quadrature squeezing of mirrors in cavity optomechanics, *Phys. Rev. A* **83**, 033820 (2011).
 - [26] G. Milburn and D. F. Walls, Production of squeezed states in a degenerate parametric amplifier, *Opt. Comm.* **39**, 401 (1981).
 - [27] A. Mari and J. Eisert, Gently Modulating Optomechanical Systems, *Phys. Rev. Lett.* **103**, 213603 (2009).
 - [28] A. Pontin, M. Bonaldi, A. Borrielli, F. S. Cataliotti, F. Marino, G. A. Prodi, E. Serra, and F. Marin, Squeezing a Thermal Mechanical Oscillator by Stabilized Parametric Effect on the Optical Spring, *Phys. Rev. Lett.* **112**, 023601 (2014).
 - [29] A. Pontin, M. Bonaldi, A. Borrielli, L. Marconi, F. Marino, G. Pandraud, G. A. Prodi, P. M. Sarro, E. Serra, and F. Marin, Dynamical Two-Mode Squeezing of Thermal Fluctuations in a Cavity Optomechanical System, *Phys. Rev. Lett.* **116**, 103601 (2016).
 - [30] A. Chowdhury, P. Vezio, M. Bonaldi, A. Borrielli, F. Marino, B. Morana, G. A. Prodi, P. M. Sarro, E. Serra, and F. Marin, Quantum Signature of a Squeezed Mechanical Oscillator, *Phys. Rev. Lett.* **124**, 023601 (2020).
 - [31] Y. Li, A.-N. Xu, L.-G. Huang, and Y.-C. Liu, Mechanical squeezing via detuning-switched driving, *Phys. Rev. A*

- 107, 033508 (2023).**
- [32] A. A. Clerk, F. Marquardt, and K. Jacobs, Back-action evasion and squeezing of a mechanical resonator using a cavity detector, *New J. Phys.* **10**, 095010 (2008).
 - [33] A. Szorkovszky, A. C. Doherty, G. I. Harris, and W. P. Bowen, Mechanical Squeezing via Parametric Amplification and Weak Measurement, *Phys. Rev. Lett.* **107**, 213603 (2011).
 - [34] G. Vasilakis, H. Shen, K. Jensen, M. Balabas, D. Salart, B. Chen, and E. S. Polzik, Generation of a squeezed state of an oscillator by stroboscopic back-action-evading measurement, *Nat. Phys.* **11**, 389 (2015).
 - [35] C. Meng, G. A. Brawley, J. S. Bennett, M. R. Vanner, and W. P. Bowen, Mechanical Squeezing via Fast Continuous Measurement, *Phys. Rev. Lett.* **125**, 043604 (2020).
 - [36] J.-M. Pirkkalainen, E. Damskäg, M. Brandt, F. Massel, and M. A. Sillanpää, Squeezing of Quantum Noise of Motion in a Micromechanical Resonator, *Phys. Rev. Lett.* **115**, 243601 (2015).
 - [37] K. Jähne, C. Genes, K. Hammerer, M. Wallquist, E. S. Polzik, and P. Zoller, Cavity-assisted squeezing of a mechanical oscillator, *Phys. Rev. A* **79**, 063819 (2009).
 - [38] G. S. Agarwal and S. Huang, Strong mechanical squeezing and its detection, *Phys. Rev. A* **93**, 043844 (2016).
 - [39] J. Huang, D.-G. Lai, and J.-Q. Liao, Controllable generation of mechanical quadrature squeezing via dark-mode engineering in cavity optomechanics, *Phys. Rev. A* **108**, 013516 (2023).
 - [40] M. Asjad, G. S. Agarwal, M. S. Kim, P. Tombesi, G. D. Giuseppe, and D. Vitali, Robust stationary mechanical squeezing in a kicked quadratic optomechanical system, *Phys. Rev. A* **89**, 023849 (2014).
 - [41] X.-Y. Lü, J.-Q. Liao, L. Tian, and F. Nori, Steady-state mechanical squeezing in an optomechanical system via Duffing nonlinearity, *Phys. Rev. A* **91**, 013834 (2015).
 - [42] M. Rashid, T. Tufarelli, J. Bateman, J. Vovrosh, D. Hempston, M. S. Kim, and H. Ulbricht, Experimental Realization of a Thermal Squeezed State of Levitated Optomechanics, *Phys. Rev. Lett.* **117**, 273601 (2016).
 - [43] A. Kronwald, F. Marquardt, and A. A. Clerk, Arbitrarily large steady-state bosonic squeezing via dissipation, *Phys. Rev. A* **88**, 063833 (2013).
 - [44] B. Xiong, X. Li, S. L. Chao, and L. Zhou, Optomechanical quadrature squeezing in the non-Markovian regime, *Opt. Lett.* **43**, 6053 (2018).
 - [45] S. L. Braunstein and P. van Loock, Quantum information with continuous variables, *Rev. Mod. Phys.* **77**, 513 (2005).
 - [46] P. D. Drummond and Z. Ficek, *Quantum Squeezing* (Berlin, Heidelberg, New York, Springer-Verlag) (2004).
 - [47] C. M. Caves, K. S. Thorne, R. W. P. Drever, V. D. Sandberg, and M. Zimmermann, On the measurement of a weak classical force coupled to a quantum-mechanical oscillator. I. Issues of principle, *Rev. Mod. Phys.* **52**, 341 (1980).
 - [48] M. O. Scully and M. S. Zubairy, *Quantum Optics* (Cambridge University Press, Cambridge, England, 1997).
 - [49] M. R. Vanner, I. Pikovski, G. D. Cole, M. S. Kim, C. Brukner, K. Hammerer, G. J. Milburn, and M. Aspelmeyer, Pulsed quantum optomechanics, *Proc. Natl. Acad. Sci.* **108**, 16182 (2011).
 - [50] M. R. Vanner, J. Hofer, G. D. Cole, and M. Aspelmeyer, Cooling-by-measurement and mechanical state tomography via pulsed optomechanics, *Nat. Commun.* **4**, 2295 (2013).
 - [51] S. M. Meenehan, J. D. Cohen, G. S. MacCabe, F. Marsili, M. D. Shaw, and O. Painter, Pulsed Excitation Dynamics of an Optomechanical Crystal Resonator near Its Quantum Ground State of Motion, *Phys. Rev. X* **5**, 041002 (2015).
 - [52] S. G. Hofer and K. Hammerer, Quantum Control of Optomechanical Systems, *Adv. At. Mol. Opt. Phys.* **66**, 263 (2017).
 - [53] Y. Wang, J.-L. Wu, Y.-K. Feng, J.-X. Han, Y. Xia, Y.-Y. Jiang, and J. Song, Optimal Control for Robust Photon State Transfer in Optomechanical Systems, *Ann. Phys. (Berlin)* **553**, 2000608 (2021).
 - [54] X. Wang, S. Vinjanampathy, F. W. Strauch, and K. Jacobs, Ultraefficient Cooling of Resonators: Beating Sideband Cooling with Quantum Control, *Phys. Rev. Lett.* **107**, 177204 (2011).
 - [55] F. Tebbenjohanns, M. L. Mattana, M. Rossi, M. Frimmer, and L. Novotny, Quantum control of a nanoparticle optically levitated in cryogenic free space, *Nature (London)* **595**, 378 (2021).
 - [56] Y.-H. Liu, X.-L. Yin, J.-F. Huang, and J.-Q. Liao, Accelerated ground-state cooling of an optomechanical resonator via shortcuts to adiabaticity, *Phys. Rev. A* **105**, 023504 (2022).
 - [57] D. Stefanatos, Maximising optomechanical entanglement with optimal control, *Quantum Sci. Technol.* **2**, 014003 (2017).
 - [58] J. Clarke, P. Sahium, K. Khosla, I. Pikovski, M. Kim, and M. Vanner, Generating mechanical and optomechanical entanglement via pulsed interaction and measurement, *New J. Phys.* **22**, 063001 (2020).
 - [59] D. Basilewitsch, C. P. Koch, and D. M. Reich, Quantum Optimal Control for Mixed State Squeezing in Cavity Optomechanics, *Adv. Quantum Technol.* **2**, 1800110 (2019).
 - [60] B. Xiong, L. Xun, S.-L. Chao, Z. Yang, W.-Z. Zhang, W. Zhang, and L. Zhou, Strong mechanical squeezing in an optomechanical system based on Lyapunov control, *Photon. Res.* **8**, 151 (2020).
 - [61] D. Dong, and I. R. Petersen, *Learning and Robust Control in Quantum Technology*, (Springer Nature, Switzerland AG, 2023).
 - [62] G. S. Agarwal, *Quantum Optics* (Cambridge University Press, Cambridge, 2013).
 - [63] W. Vogel and D. Welsch, *Quantum Optics* (Wiley-VCH, Weinheim, 2006).
 - [64] We checked the correctness of the pulsed fields by back-substituting the pulsed field data obtained after the last iteration into the system evolution. We verified the results by either solving the covariance matrix \mathbf{V} or solving the quantum master equation (4) under the replacement of $H_{\text{dis}}(t) \rightarrow H_{\text{lin}}(t)$. We find that the dynamic evolution of the squeezing degree \mathcal{S}_b are consistent with the results obtained in this paper.
 - [65] Y. S. Park and H. Wang, Resolved-sideband and cryogenic cooling of an optomechanical resonator, *Nat. Phys.* **5**, 489 (2009).
 - [66] A. Schliesser, O. Arcizet, R. Rivière, G. Anetsberger, and T. J. Kippenberg, Resolved-sideband cooling and position measurement of a micromechanical oscillator close to the Heisenberg uncertainty limit, *Nat. Phys.* **5**, 509 (2009).
 - [67] E. Verhagen, S. Deléglise, S. Weis, A. Schliesser, and T. J.

- Kippenberg, Quantum-coherent coupling of a mechanical oscillator to an optical cavity mode, *Nature (London)* **482**, 63 (2012).
- [68] J. B. Hertzberg, T. Rocheleau, T. Ndukum, M. Savva, A. A. Clerk, and K. C. Schwab, Back-action-evading measurements of nanomechanical motion, *Nat. Phys.* **6**, 213 (2010).
- [69] F. Massel, T. T. Heikkilä, J.-M. Pirkkalainen, S. U. Cho, H. Saloniemi, P. J. Hakonen, and M. A. Sillanpää, Microwave amplification with nanomechanical resonators, *Nature (London)* **480**, 351 (2011).
- [70] F. Massel, S. U. Cho, J.-M. Pirkkalainen, P. J. Hakonen, T. T. Heikkilä, and M. A. Sillanpää, Multimode circuit optomechanics near the quantum limit, *Nat. Commun.* **3**, 987 (2012).
- [71] M. Eichenfield, R. Camacho, J. Chan, K. J. Vahala, and O. Painter, A picogram- and nanometre-scale photonic-crystal optomechanical cavity, *Nature (London)* **459**, 550 (2009).
- [72] M. Eichenfield, J. Chan, R. M. Camacho, K. J. Vahala, and O. Painter, Optomechanical crystals, *Nature (London)* **462**, 78 (2009).
- [73] S. Gröblacher, K. Hammerer, M. R. Vanner, and M. Aspelmeyer, Observation of strong coupling between a micro-mechanical resonator and an optical cavity field, *Nature (London)* **460**, 724 (2009).
- [74] W. Greiner and J. Reinhardt, *Field Quantization* (Springer, Berlin, 1996).